Supporting Information

Scalable Solvothermal Synthesis of Superparamagnetic Fe_3O_4 Nanoclusters for bio-separation and theragnostic probes

Jeonghyo Kim[1, †], Van Tan Tran[1, †], Sangjin Oh[1, †], Chang-Seok Kim[1], Jong Chul Hong[2], SungIl Kim[3], Young-Seon Joo[3], Saem Mun[3], Myoung-Ho Kim[3], Jae-Wan Jung[3], Jiyoung Lee[4], Yong Seok Kang[4], Ja-Won Koo[4], Jaebeom Lee[5,]*

[1]Departments of Cogno-Mechatronics Engineering, Pusan National University, Busan, 46241, Republic of Korea

[2]Department of Otolaryngology, Head and Neck Surgery, College of Medicine, Dong-A University, Busan, 49201, Republic of Korea

[3]AMO LIFE SCIENCE Co., Ltd., Seoul, 06527, Republic of Korea

[4]Department of Otorhinolaryngology-Head and Neck Surgery, Seoul National University Bundang Hospital, Seongnam, 13620, Republic of Korea

[5]Department of Chemistry, Chungnam National University, Daejeon, 34134, Republic of Korea

[†]These authors contributed equally.

*Corresponding author
Email: nanoleelab@cnu.ac.kr

TABLE OF CONTENTS

Table S1. Reaction conditions for size tunability evaluation.

	Conc. of $FeCl_3$ (M)	Reaction volume (mL)	Na_3Cit (g)	NaAc (g)	Reaction Temp. (°C)	Reaction Time (h)
a	0.05	20	0.2	1.2	200°C	10
b	0.1	20	0.2	1.2	200°C	10
c	0.2	20	0.2	1.2	200°C	10
d	0.3	20	0.2	1.2	200°C	10

Table S2. Reaction conditions for scalability evaluation.

Reaction volume (mL)	Amount of $FeCl_3$ (g)	Conc. of $FeCl_3$ (M)	Na_3Cit (g)	NaAc (g)	Reaction Temp. (°C)	Reaction Time (h)
20	0.540	0.1	0.2	1.2	200°C	10
40	1.081	0.1	0.4	2.4	200°C	10
200	5.406	0.1	2	12	200°C	10

Table S3. Quantification of conjugated-antibody amount.

	OD@562 nm (a.u.)	Conjugated-antibody amount/1 mg of particles (μg)
Anti-RBC antibody	0.416	30.7
Anti-CRP antibody	0.413	30.5
Anti-Vibrio antibody	0.471	35

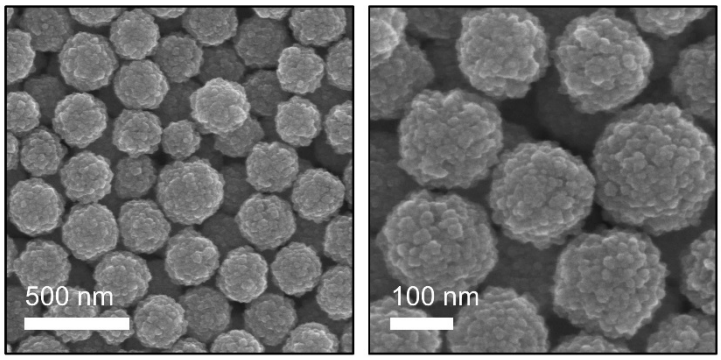

Figure S1. Representative SEM images of the fabricated Fe_3O_4 nanoclusters at different magnifications.

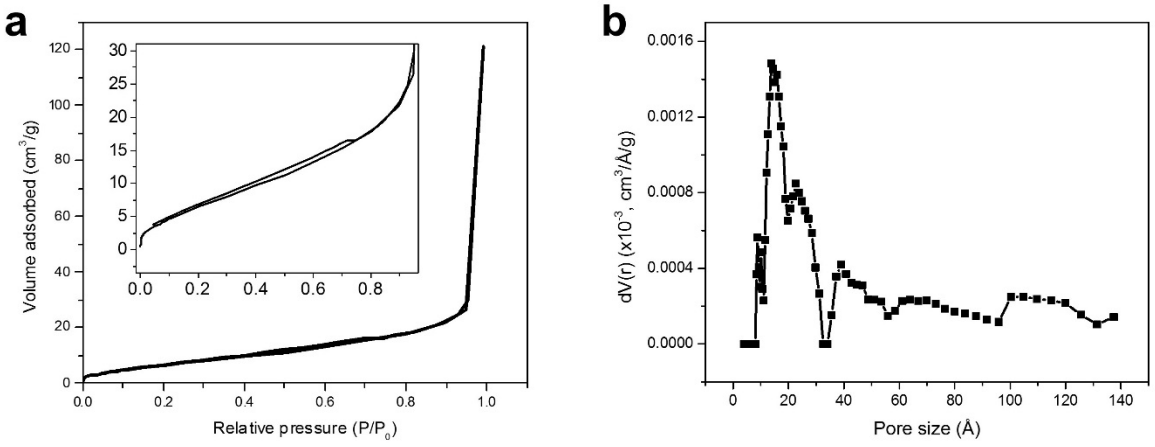

Figure S2. (a) The nitrogen adsorption-desorption isotherm, and (b) pore size distribution curve of MNCs.

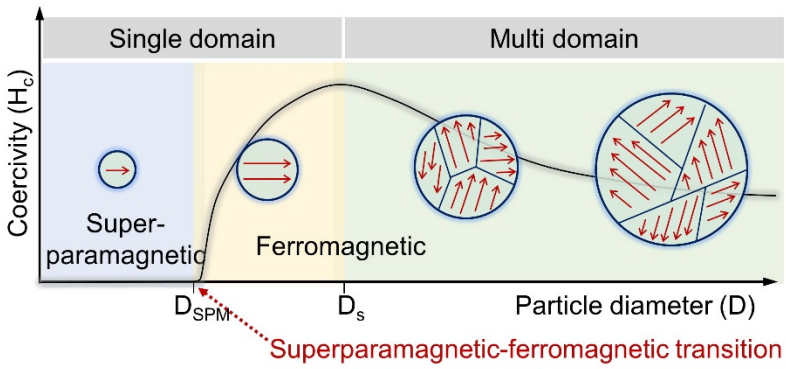

Figure S3. Schematic diagram of the coercivity (H_c) behavior as a function of particle diameter (D), where D_s is the diameter at which a transition from multi-domain to single-domain occurs, and D_{SPM} is the zero-coercivity diameter.

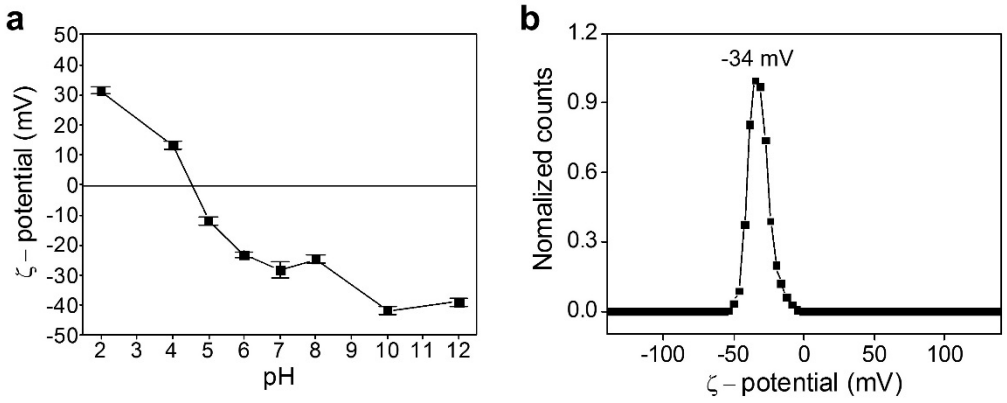

Figure S4. (a) pH-dependent zeta-potential curves, and (b) Zeta-potential of MNCs in aqueous dispersions.

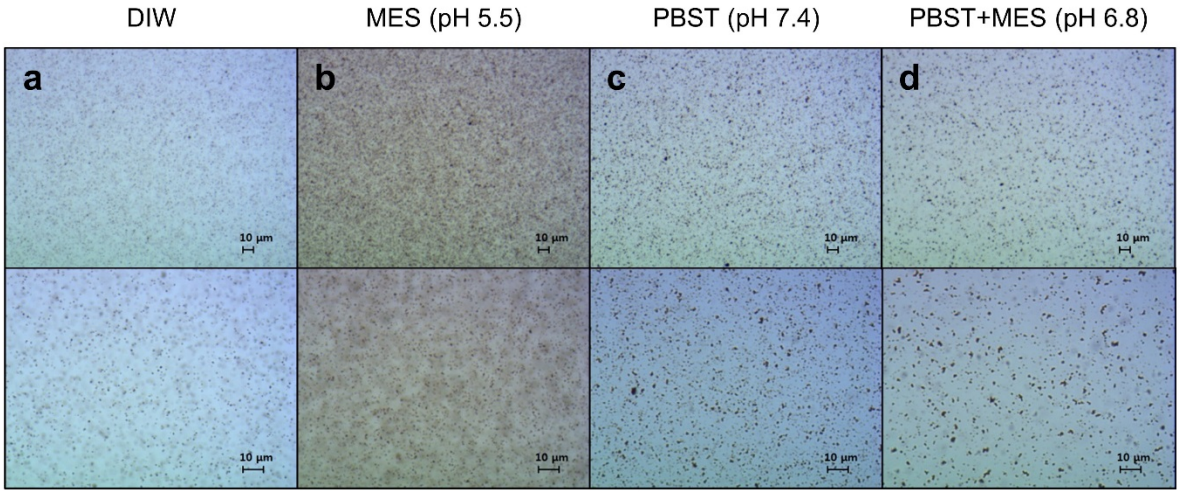

Figure S5. Optical microscopy images of magnetic nanoclusters (MNCs) in different buffer solutions: (a) deionized water (DIW), (b) MES (pH 5.5), (c) phosphate buffered saline with Tween-20 (PBST, pH 7.4), and (d) mixture of PBST and MES (pH 6.8).

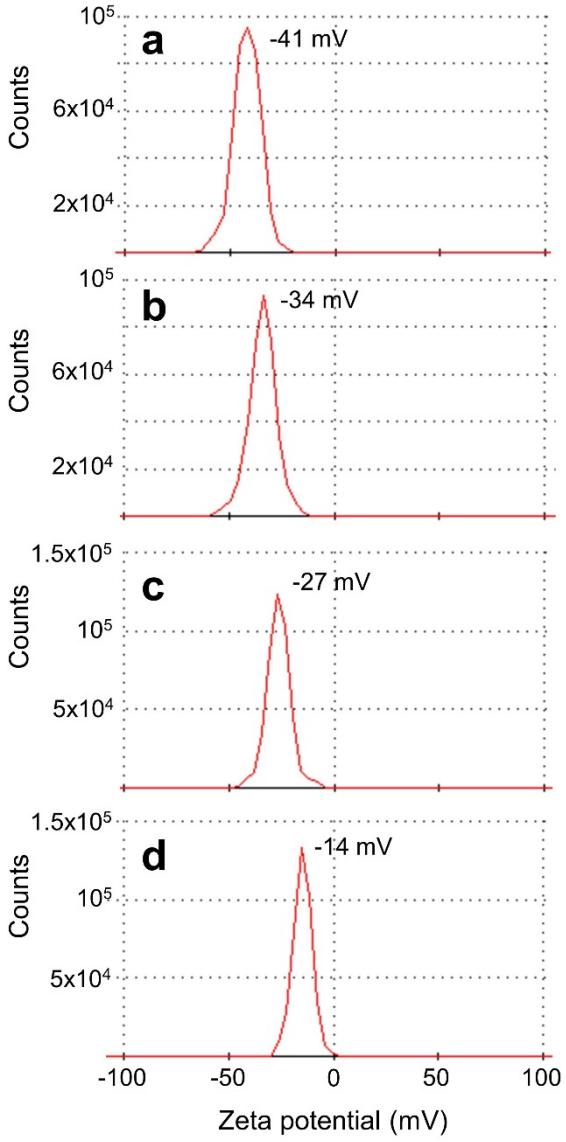

Figure S6. Zeta-potentials of the Fe_3O_4 nanospheres synthesized with a Fe precursor concentration of 0.05 M (a), 0.1 M (b), 0.2 M (c), and 0.3 M (d).

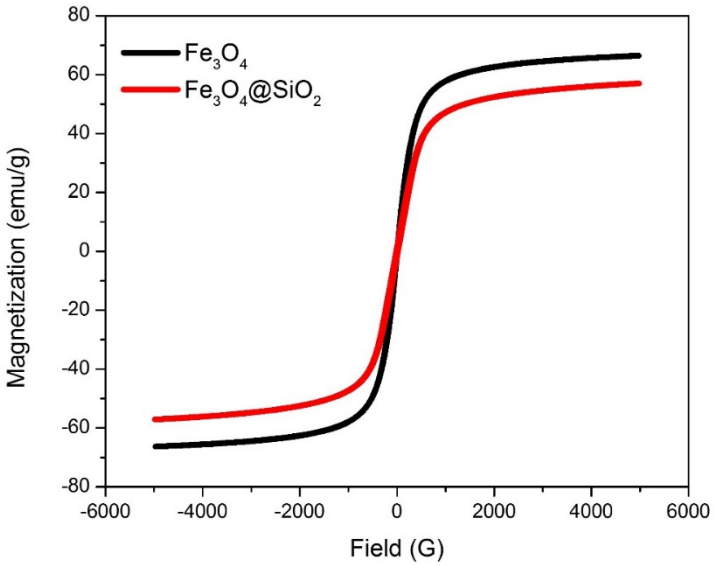

Figure S7. Magnetization curves of Fe_3O_4 and $Fe_3O_4@SiO_2$ samples measured at 300 K.

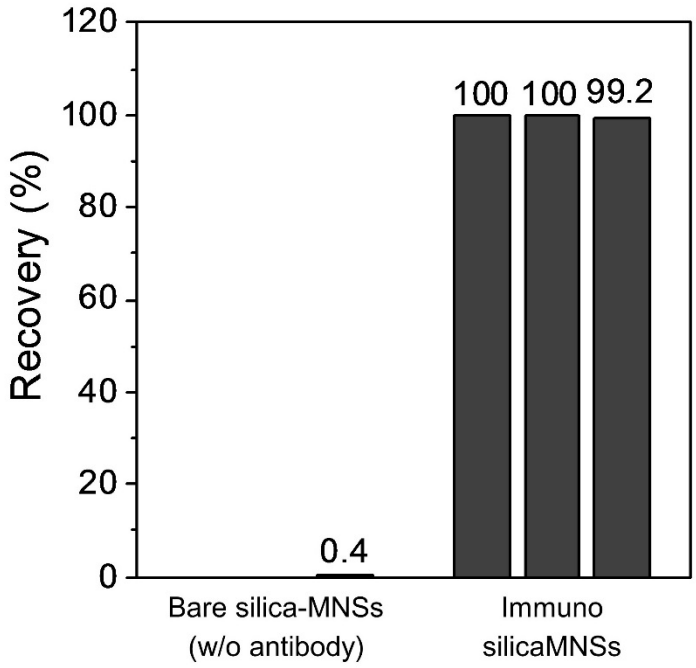

Figure S8. Capture efficiency of Ab-conjugated silica-MNSs for vibrio cell samples.

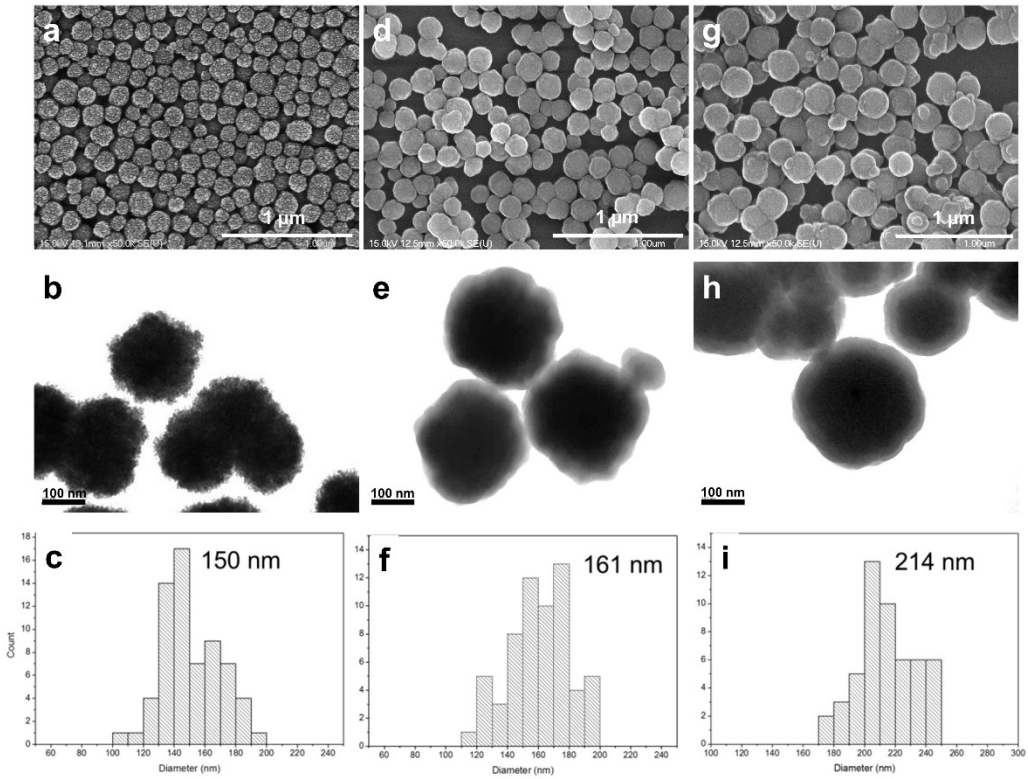

Figure S9. SEM, TEM and size distribution histogram of (a-c) Fe_3O_4, (d-f) Fe_3O_4@SiO_2, and (g-i) Eu doped Fe_3O_4@SiO_2. Size distribution of nanoclusters obtained by measuring 100 particles from TEM images.

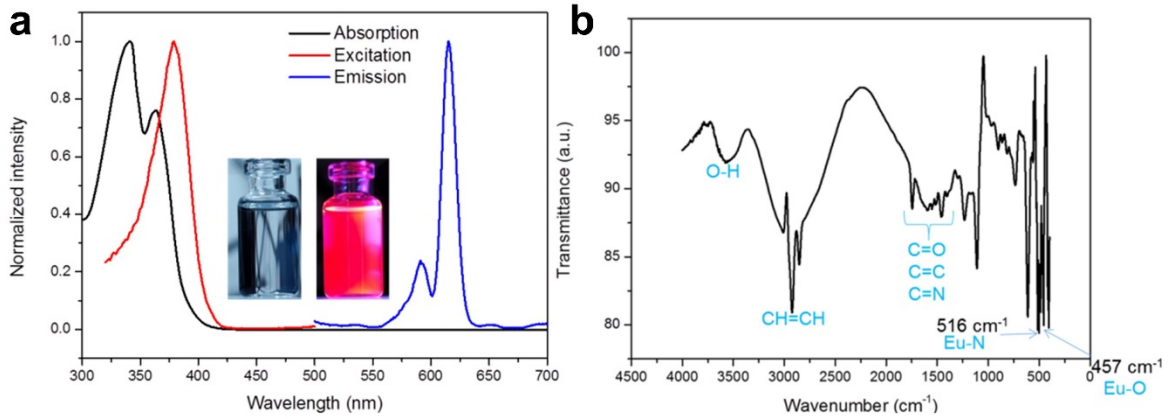

Figure S10. (a) Absorption, excitation and emission spectra of $Eu(DBM)_3Phen$, and (b) its FT-IR spectrum.

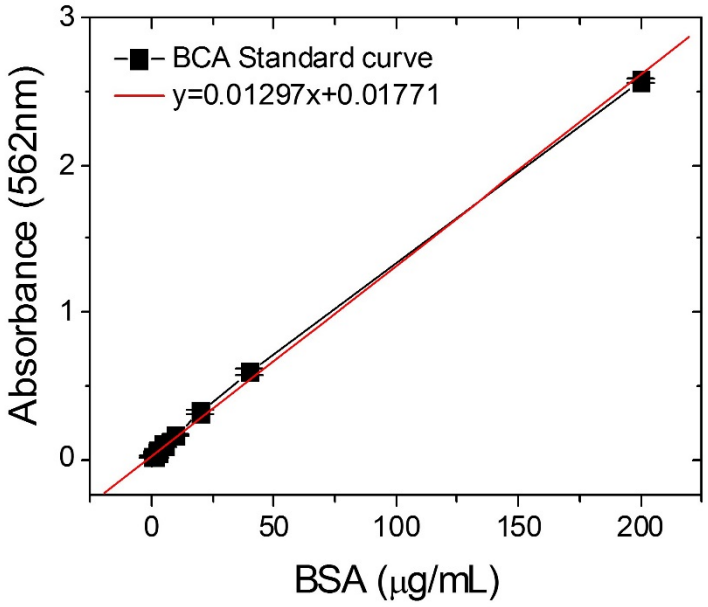

Figure S11. Bovine serum albumin (BSA) standard curve for the BCA protein assay.

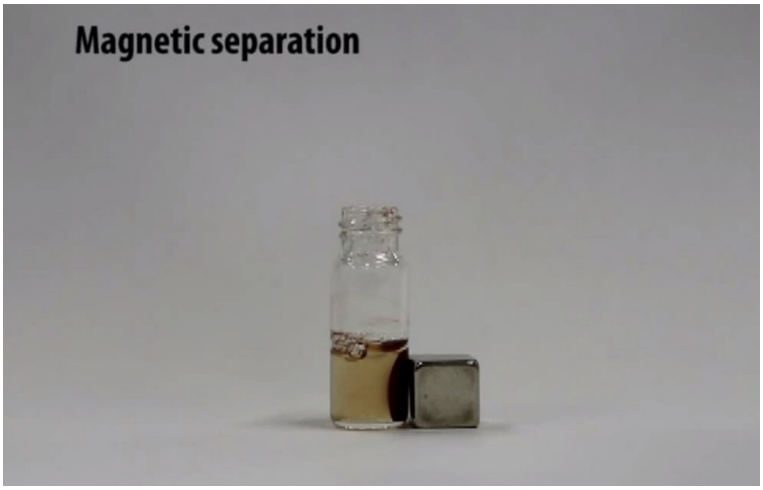

Supplementary Movie S1. Video clip showing the RBC separation from human whole blood.